BRAPH: A TOOLBOX DEVELOPED FOR BRAIN GRAPH ANALYSIS OF VARIOUS IMAGING MODALITIES

A THESIS SUBMITTED TO

THE GRADUATE SCHOOL OF ENGINEERING AND SCIENCE

OF BILKENT UNIVERSITY

IN PARTIAL FULFILLMENT OF THE REQUIREMENTS FOR

THE DEGREE OF

MASTER OF SCIENCE

IN

PHYSICS

By

Ehsan Kakaei

March 2017

BRAPH: A TOOLBOX DEVELOPED FOR BRAIN GRAPH ANALYSIS OF VARIOUS IMAGING MODALITIES
By Ehsan Kakaei
March 2017

We certify that we have read this thesis and that in our opinion it is fully adequate, in scope and in quality, as a thesis for the degree of Master of Science.

Giovanni Volpe(Advisor)

Balázs Hetényi

Gökhan Barış Bağcı

Approved for the Graduate School of Engineering and Science:

Ezhan Karaşan
Director of the Graduate School

ABSTRACT

BRAPH: A TOOLBOX DEVELOPED FOR BRAIN GRAPH ANALYSIS OF VARIOUS IMAGING MODALITIES

Ehsan Kakaei
M.S. in Physics
Advisor: Giovanni Volpe
March 2017

Complex systems, like the human brain, are composed of a huge number of interacting elements showing complex patterns. Graph theory provides a mathematical toolbox for investigating the role of each element in these systems. With the rise of interest in applying this method for studying brain networks, several software have been developed to allow researches conduct brain network analysis. However, a comprehensive and an easy-to-use toolbox is still lacking. BRAPH is the first object-oriented toolbox that provides users the ability of constructing and analyzing brain networks out of data acquired from various imaging modalities. For this purpose, multiple graphical user interfaces (GUIs) have been designed that allow the users to import or build brain atlases, along with cohort of subjects, prior to starting the graph analysis. Various graph measures for both weighted graphs and binary graphs, comparison between groups, comparison with random graphs, longitudinal analysis and statistical analysis, are only some of the analysis tools embedded in BRAPH.

Keywords: graph theory analysis, object-oriented software, network topology, longitudinal analysis.

ÖZET

BRAPH: BEYİN ÇİZGE ANALİZİNİN FARKLI GÖRÜNTÜLEME YÖNTEMLERİNE YÖNELİK GELİŞTİRİLMİŞ ARAÇ KUTUSU

Ehsan Kakaei
Fizik, Yüksek Lisans
Tez Danışmanı: Giovanni Volpe
Mart 2017

Karmaşık sistemler, insan beyni gibi, kompleks örüntüler sergileyen çok sayıda birbiriyle etkileşen elemandan oluşur. Çizge teorisi, her elemanın sistemdeki rolünü incelemek için matematiksel bir araç kutusu sunar. Bu yöntemi beyin şebekelerinde kullanmaya artan ilgiyle birlikte geliştirilen pekçok yazılım, araştırmacıların beyin şebekelerini analiz etmesinin önünü açmıştır. Ancak, kapsamlı ve kullanımı kolay olan bir araç kutusunun hala eksikliği çekilmektedir. BRAPH, kullanıcıların, beyin şebekelerinin farklı görüntüleme yöntemleriyle elde edilen verileri düzenlemesini ve analizini sağlayan ilk nesne yönelimli araç kutusudur. Bu amaçla, kullanıcıların çizge analizinin öncesinde, beyin atlaslarının kohortuyla birlikte aktarabilmelsi ya da kurabilmesi için çoklu grafksel kullanıcı arayüzleri (GUIs) tasarlanmıştır. Hem ikili hem de ağırlıklı çizgelere uygulanabilen çeşitli ölçümler, grupların karşılaştırılması, raslantısal şebekelerle karşılaştırma, boylamsal analizler ve istatistiksel analizler, BRAPH'ın içerdiği analiz araçlarından yalnızca bir kaçıdır.

Anahtar sözcükler: Çizge teori analizleri, nesne yönelimli yazılım, şebeke Topolojisi, boylamsal analizler.

Acknowledgement

First, I would like to acknowledge my advisor Prof. Giovanni Volpe who gave me the chance to start doing research in a new area and always supported and motivated me with his kind advice and brilliant ideas. His leadership taught me the importance of group work and professionalism.

I am also grateful for having a mentor like Mite Mijalkov who patiently introduced me the basic concepts of graph theory and object-oriented programming, step by step. I also appreciate Dr. Joana B. Pereira and Prof. Eric Westman for their collaboration which was essential for developing and designing the toolbox.

In addition, I want to express my joy of knowing all the members in the Soft Matter Lab and thank them for all the support they provided. Finally, I would like to appreciate my family in gratitude for their love and life-long encouragement.

Contents

1 Introduction **1**

1.1 Network and neurological disorders 2

1.2 Toolboxes 3

1.3 Scope of the thesis 3

2 Brain Graphs **5**

2.1 Graph 5

2.2 Constructing the brain graphs 9

3 Graph Analysis **14**

3.1 Graph measures 14

3.2 Statistical analysis 25

4 BRAPH **28**

4.1 Brain atlas 29

4.2 Cohort 30

4.3 Graph analysis 34

4.3.1 Pre-analysis 34

4.3.2 Analysis 37

List of Figures

2.1 A simple graph 6

2.2 Types of graphs 7

2.3 Constructing the connectivity matrix 12

3.1 Degree of a binary undirected graph 16

3.2 Shortest pathway between two nodes 17

3.3 Triangles in a binary undirected graph. 19

3.4 Closeness and betweenness centrality of the nodes 21

3.5 Modules of a graph 22

3.6 A simple binary undirected graph 24

3.7 Calculation of P-value 26

3.8 Correcting p-values due to FDR. 26

4.1 Work-flow of BRAPH 28

4.2 Brain atlas graphical user interface 29

4.3 Proper form of a Brain Atlas in xls format 30

4.4 MRI Cohort graphical user interface 31

4.5 Proper form of a group of subjects in xls format for MRI cohort . 32

4.6 Brain view menu of GUIMRICohort 32

4.7 fMRI Cohort graphical user interface 33

4.8 Proper form of a data file of a subject in xls format for fMRI cohort 33

4.9 MRI pre-analysis graphical user interface 35

4.10 fMRI pre-analysis graphical user interface 36

4.11 Graph analysis graphical user interface for weighted graphs 38

4.12 Visualization of the analysis results by brain view 39

4.13 Visualization of the analysis results for different densities 40

List of Tables

3.1 Nodal measures calculated for a simple binary undirected graph . 24

Chapter 1

Introduction

The study of the brain is not new and dates back to ancient times as old as the Neolithic era. However, modern neurophysiology only began in the late 19th and early 20th century [1] and the quantitative study of the brain is just at its early ages.

Brain consists of an enormous number of interacting elements – to be more precise, more than 10^{11} neurons [2] – which are connected to each other, forming a very dense network that shows complicated dynamics. Therefore, understanding the behavior of brain requires the knowledge of the nature of its components and their interactions and studying the macroscopic properties of the system, like every other complex systems [3].

Graph theory is a mathematical tool for analyzing the networks and provides useful information on network topology. The high sensitivity of this method to the alterations in the networks makes it a favorable technique for studying the brain network which gives an insight into the role of individual elements in the brain functions.

In this chapter, first a summary on the relation between the brain network and cognition, behavior and neurological disorders is given. Afterwards, some of the graph theoretical-based toolboxes for the brain network analysis is introduced.

Finally, the scope of this thesis is introduced.

1.1 Network and neurological disorders

As described above, network analysis of the brain provides information on topological properties of the brain and can depict both local and global pathologies. Studies on different neurological disorders by using the graph theory is done at different levels, e.g. the change in the cellular networks after Traumatic Brain Injury (TBI) [4, 5]. However, most of the studies are focused on the networks at system level and the whole-brain networks.

Biological systems are organized in such a way that their functionality comes at lowest possible cost and with highest precision. Nervous system of *Caenorhabditis elegans* is a marvelous example of such a system. The small-world characteristic of this system (high clustering and short path length) makes it an optimally-designed network [6]. This property of the network provides the functional segregation and integration at the same time which is one of the features of cognitive systems.

Many researches have shown that the small-world organization of a normal brain is altered in patients suffering from Multiple sclerosis (MS), TBI and epilepsy [7]. However, this is not the only property of the brain network that is changed and other distortions in the network can be indicated by comparing different graph measures between healthy controls and group of patients (see chapter 3). For example, increased modality and path length and decreased transitivity in a group of patients with Alzheimer's disease (AD) and a group of subjects with mild cognitive impairment (MCI) – which is a transition state from normal to AD – is shown; as well as increased characteristic path length and reducted global efficiency for patients with Parkinson's disease with mild cognitive impairment (PD-MCI) [8, 9].

1.2 Toolboxes

With the increase of interest in applying the graph theory for brain network analysis, a comprehensive toolbox capable of analyzing brain networks is in demand. For this purpose, several toolboxes have been developed to cover this need. The *brain-connectivity-toolbox* (BCT) [10] is one of the early toolboxes that have been developed and contains majority of the measures and analysis tools that have been used in most of the later toolboxes. However, this toolbox requires programming skills and is not very user-friendly.

In recent years, lots of toolboxes [11, 12, 13, 14, 15, 16] have been developed to solve this problem. Even though these toolboxes contain graphical user interfaces (GUIs), they are either not comprehensive toolboxes and lack some parts of analysis or they are not adaptable and are not easy to use. Therefore, still the need for accessing a user-friendly and comprehensive toolbox is not fulfilled.

In this thesis, we are introducing BRAPH – BRain Analysis using graPH theory – as a MATLAB-based toolbox capable of analyzing the brain networks constructed out of various imaging modalities with easy-to-use GUIs. This toolbox is the first object-oriented toolbox which makes the upgrade and adaptation of it easier. In addition, BRAPH provides longitudinal analysis to study variation in the topology of networks over time. Finally, a complete manual and online tutorial videos have made the dealing with this toolbox easier for users.

1.3 Scope of the thesis

Before introducing BRAPH, first an introduction on the graph theory, different types of the graphs, and means of constructing graphs out of different data types acquired by various imaging modalities is given in the *Chapter 2*. Then, mathematical tools for graph analysis (i.e. graph measures and statistical analysis) are discussed in the *Chapter 3*. Finally, different graphical user interfaces of BRAPH for creating and modifying brain atlases, cohort of subjects and graph analysis

are presented in the *Chapter 4*.

Chapter 2

Brain Graphs

To perform graph analysis on brain networks, constructing a well-defined brain graph is inevitable. For this purpose, different types of graphs and their representations are introduced. Later, a procedure for constructing these graphs out of different imaging modalities is provided.

2.1 Graph

A graph consistes of a set of elements (*nodes*) and *edges* and a relation that assignes each edge to a pair of nodes [17]. A graphical representation of a simple graph is given in the figure 2.1 in which every node and edge is represented by a sphere and an arrow, respectively. However, this representation is not suitable for illustrating the complex networks with a large number of nodes and edges and calculating the graph measures.

A possible solution for this problem is the use of *connectivity matrix*. The connectivity matrix representing a graph is a square $N \times N$ matrix where N is the number of nodes. The (i, j) element of the matrix represents the edge starting from the node i to the node j. As an example, the connectivity matrix for the graph shown in the figure 2.1 is:

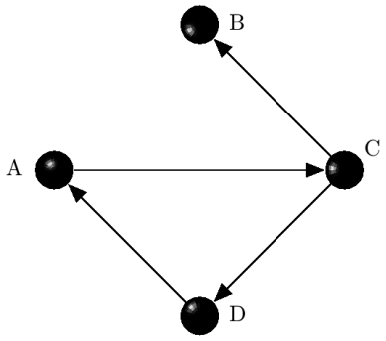

Figure 2.1: A simple graph. The nodes are shown as spheres and the edges are depicted as arrows.

$$A = \begin{bmatrix} 0 & 0 & 1 & 0 \\ 0 & 0 & 0 & 0 \\ 0 & 1 & 0 & 1 \\ 1 & 0 & 0 & 0 \end{bmatrix}$$

where the incoming (outgoing) edges of the nodes A, B, C and D are shown in the columns (rows) 1 to 4.

Types of graphs

A graph can be categorized based on the nature of its edges. A graph can be either *directed* or *undirected* in the sense of the direction of the edges. In addition, the edges can be either *weighted* or *binary* (Fig. 2.2).

In the case of the binary graphs, every pair of nodes are either connected or not (0 or 1). On the other hand, in the weighted graphs a weight is assigned to each edge which can get any value in the range $[-1, 1]$ (if the weights are normalized). However, we will consider the weights as non-negative numbers, in most cases.

If the edges between two nodes have a certain direction, the graph is a directed graph. Otherwise, the graph is an undirected one. The connectivity matrix of an undirected graph is symmetric, since $A_{ij} = A_{ji}$.

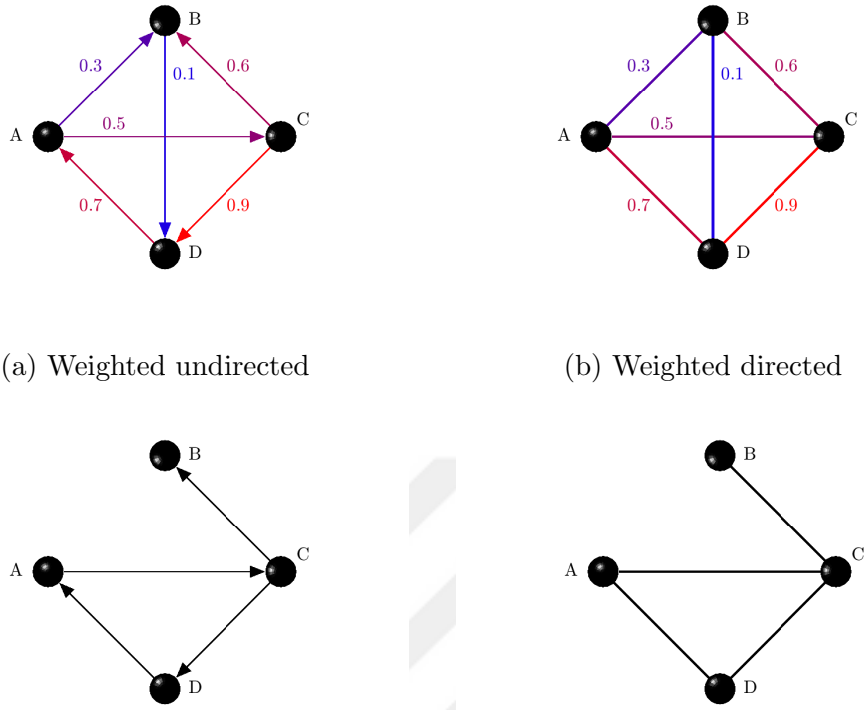

(a) Weighted undirected

(b) Weighted directed

(c) Binary directed

(d) Binary undirected

Figure 2.2: Different types of graphs are illustrated. In order to generate the binary graphs (c) and (d) out of the weighted graphs (a) and (b), a threshold of 0.4 has been assumed. By doing so, the $A \leftrightarrow B$ and $B \leftrightarrow D$ edges have been eliminated. To turn the directed graphs (a) and (c) into the undirected graphs (b) and (d), the maximum-weight method has been used.

It is possible to convert weighted graphs into binary graphs and directed graphs into the undirected graphs (but the opposite is not possible).

The conversion from the weighted graphs into the binary ones can be achieved by the binarization process. This process is done by assuming a *threshold*. If the weight of an edge is below the threshold, the nodes to which the edge is assigned, are considered as disconnected. For example, if we assume the threshold to be 0.4 in the weighted graphs shown in the figure 2.2 the edges between nodes $A \leftrightarrow B$ and $B \leftrightarrow D$ will be eliminated and the graphs **a** and **b** would turn into the graphs**c** and **d**, respectively.

The other desired conversion between graphs of different types, is the conversion from the directed graphs into the undirected graphs. This objective can be reached by the *symmetrization* of the connectivity matrix. Since the A_{ij} and

A_{ji} represent the edges of opposite directions, the transposed connectivity matrix represents a directed graph with opposite directions relative to the original matrix. The symmetrization of the connectivity matrix is done by considering this fact and by applying one of the following methods:

1. **Summation method:** The connectivity matrix of an undirected graph is given by summing the connectivity matrix of the directed graph and the transposed matrix.

   $$A'_{ij} = A_{ij} + A^t_{ij}$$

   Here, A' and A are the connectivity matrices of the undirected and directed graphs, respectively.

2. **Averaging method:** The connectivity matrix of an undirected graph is given by averaging the connectivity matrix of the directed graph and the transposed matrix.

   $$A'_{ij} = \frac{A_{ij} + A^t_{ij}}{2}$$

3. **Minimum-weight method:** First, the connectivity matrix of the directed graph and its transpose are compared element wise. Then the minimum value is assigned to the connectivity matrix of the undirected graph.

   $$A'_{ij} = min(A_{ij}, A^t_{ij})$$

4. **Maximum-weight method:** First, the connectivity matrix of the directed graph and its transpose are compared element wise. Then the maximum value is assigned to the connectivity matrix of the undirected graph.

   $$A'_{ij} = max(A_{ij}, A^t_{ij})$$

2.2 Constructing the brain graphs

The construction of the brain graphs depends on the type of the imaging modality that we are dealing with, since the methods used for defining the nodes and edges in *structural* and *functional* imaging modalities are different.

In this section, an overview of the procedures for defining the nodes and edges for different kinds of imaging modalities will be provided. Afterward, the construction of the connectivity matrix for different imaging techniques – for which the BRAPH is designed – will be discussed.

Defining the nodes

Usually, the nodes in the brain graphs represent brain regions. The selection of the brain regions depends on the parcellation and the brain mapping methods used for different imaging modalities. Therefore, the selection of the nodes are not unique. Different nodes selections would result in different network topologies [18].

In BRAPH the node selection process can be done in GUIBrainAtlas by adding, editing or creating different atlases, such as AAL90 [19], Dosenbach [20] and Desikan [21]. We will discuss this procedure in more details in the chapter 4.

Defining the edges

As discussed above, the nodes in the brain graphs represent the brain regions. The edges between each pair of nodes represent the anatomical or functional connectivity between them. The edges are defined based on the correlation between each pair of nodes either within group (in the case of MRI and static PET) or between their time series for each subject (in the case of fMRI and EEG).

Correlation functions

Previously, we discussed that a edges in a graph is defined by finding the correlation between data of the nodes to which it has been assigned. In BRAPH we use the following correlation functions in order to define edges:

- **Pearson correlation:** This correlation coefficient represents how two variables are linearly dependent to each other, and can be calculated by:

  $$\rho = \frac{\sigma_{xy}}{\sigma_x \sigma_y}$$

  where σ_{xy} is the covariance of the variables x and y, and σ_x and σ_y is their standard deviation.

  The range of the values of this correlation coefficient is $[-1, 1]$. A correlation coefficient of -1 $(+1)$ means, as a variable increase the other variable (also) decreases (increases). The correlation of 0 states that the relation between two variable is not linear and does not indicate that there is no correlation between two variables.

- **Spearman rank correlation:** If the relation between two variables is not linear, calculation of this correlation might be helpful. This correlation coefficient measures the monotonic relation between two ranked variables. In general, if the correlation coefficient is close to $+1$ (-1), for any two points (x_i, y_i) and (x_j, y_j) given $x_i > x_j$ one can deduce that $y_i > y_j$ $(y_i < y_j)$, i.e. the points are *concordant* (*discordant*).

- **Kendall rank correlation:** Kendall rank correlation provides another measure of monotonicity by comparing number of concordant and discordant pair of points with respect to the total possible number of pairs. This correlation is calculated as follows:

  $$\tau = (c - d) / \binom{n}{2}$$

  c and d are the number of concordant and discordant pair of points, respectively.

- **Partial correlation:** The correlation between two variables x and y can be resulted from the presence of a third variable z. In order to control effect of this variable the partial correlation coefficients should be calculated.

  If there is a linear relation between variables z and x, and z and y, then the regression model states that:

$$x = \alpha_0 + \alpha_1 z + \epsilon_x$$

$$y = \beta_0 + \beta_1 z + \epsilon_y$$

  where ϵ_x and ϵ_y are the parts of the model that are uncorrelated with z. Then, the partial correlation coefficient can be calculated by:

$$\rho_{xy.z} = \frac{Cov(\epsilon_x, \epsilon_y)}{\sigma_{\epsilon_x}\sigma_{\epsilon_y}}$$

  where $Cov(\epsilon_x, \epsilon_y)$ is the covariance of the ϵ_x and ϵ_y, and σ_{ϵ_x} and σ_{ϵ_y} are the standard deviations of them [22].

Connectivity matrix of the MRI data

Magnetic resonance imaging (*MRI*) is a relatively safe "non-invasive" imaging technique that is based on the magnetic property of the nucleus – hydrogen nucleus is the most dominant one – in a tissue molecule. Different tissues in the brain have different compositions and concentration of hydrogen protons, hence different magnetic properties. Therefore, by detecting the spatial variation of the MR signals, due to variation in magnetic field, the types of tissues and their relative amount can be defined [23].

T1-weighted image is one of the mostly used images obtained with MRI. In order to be able to construct the connectivity matrix out of MRI images, first these type of image should be preprocessed by other software – such as FreeSurfer [24] – to correct the artifacts, segment the tissues and normalize it to a template. Then a certain property of every region – e.g. cortical thickness, subcortical volume – should be extracted for every subject. Finally a statistical correlation between

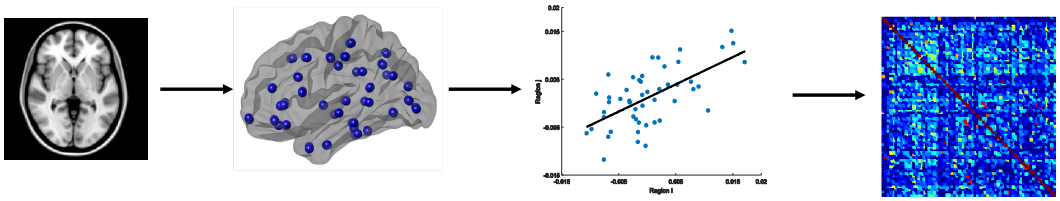

Figure 2.3: The general construction procedure of the connectivity matrix. First, the preprocessed imaging data is extracted. Then the brain atlas is constructed based on the preprocessing procedure and the data are assigned to each region. Afterwards, a correlation between data of each pair of regions are calculated. Finally, the connectivity matrix of each group or subject is constructed.

every two regions, which are the nodes of the brain graph, over each group of subjects should be calculated to generate the weight of the connection between them (Fig. 2.3).

For this imaging technique, only a single connectivity matrix will be constructed for every group of subjects and the graph measures and the comparison between different groups will be done based on them.

Connectivity matrix of the fMRI data

Neural activity requires energy consumption which is supplied via blood. Therefore, when an area of the brain increases its activity, the oxygen and glucose levels significantly change in that area. This phenomenon provides a method of measuring the relative neural activity in the brain.

Functional magnetic resonance imaging (*fMRI*) is an imaging technique that is based on the blood-oxygen-level-dependent (*BOLD*) contrast. Since oxygenated hemoglobin (Hb) and deoxygenated hemoglobin (dHb) have different magnetic properties (Hb is diamagnetic while the dHb is paramagnetic), their relative amounts result in alteration of MR signals. The change in the activity of the brain, also changes its hemodynamics, and leads to the detection of the active areas [25].

For this imaging technique, a connectivity matrix can be constructed for every subject by finding the temporal correlation between each pair of regions. Therefore, it is necessary to calculate the graph measures for each subject separately and average it for each group of subjects.

Connectivity matrix of the PET data

As mentioned before, the changes in the activity of the brain regions alters the hemodynamics of the brain and leads to the variation in the oxygen and glucose levels. Similar to fMRI, positron emission tomography (PET) is based on these changes. PET can measure both oxygen consumption and glucose utilization in brain by detecting the changes in the concentration of the radioactive compounds [26].

PET can provide both temporal and spatial patterns of the brain depending on whether we are dealing with the static imaging or the dynamic imaging technique. In BRAPH, we have implemented the graph analysis only for the static PET. The construction of the connectivity matrix for this method is similar to MRI.

Connectivity matrix of the EEG data

Electroencephalography (EEG) is a non-invasive imaging technique that measures the electrical currents on the scalp generated by a large group of neurons due to their activities and has a very high temporal resolution (unlike its spatial resolution). The procedure of the construction of the connectivity matrix for this imaging technique is similar to fMRI and they only differ in the way the nodes are defined. The nodes in fMRI portray the regions of the brain while the nodes in EEG represent the electrodes placed on the scalp.

Chapter 3

Graph Analysis

In the previous chapter we discussed the different types of graphs and their representations by adjacency matrices. In this chapter we are going to explain the different measures and methods of graph analysis mostly used in brain network science. In the first part the graph measures will be discussed in detail while the statistical analysis will be presented afterwards.

3.1 Graph measures

In general the graph measures are categorized into two major groups of *global* and *nodal* measures. A measure is a nodal measure if it quantifies a certain characteristic of every node. On the other hand, the measures which describe the properties of the whole network with a single number are considered as global measures.

Note that the values of the nodal and global measures corresponding to a simple binary undirected graph(Fig. 3.6) is indicated in the table 3.1.

Degree

Degree is the total number of edges connected to a node, i.e. number of neighboring nodes, which is a nodal measure (Fig. 3.1). For binary undirected graphs, the degree D of the node i is calculated as

$$D_i = \sum_j a_{ij} \tag{3.1}$$

where a_{ij} is the weight of the connection from the node i to the node j. Since the adjacency matrix of an undirected graph is symmetric, degree can be also calculated by summing over a_{ji}.

For directed graph, the total number of the incoming/outgoing edges to/from a node is defined as *in-degree*/*out-degree* and the degree is computed as the sum of the in-degree and out-degree.

$$D_i^{out} = \sum_j a_{ij} \tag{3.2}$$

$$D_i^{in} = \sum_j a_{ji} \tag{3.3}$$

$$D_i = D_i^{in} + D_i^{out} \tag{3.4}$$

If the graph is a weighted one, all the weight are ignored and all the non-zero weighted edges are considered as a connection.

Average degree, *average in-degree* and *average out-degree* are three global measures which are calculated as the average value of the degree, in-degree and out-degree of all nodes in the network, respectively.

Strength

Strength is a nodal measure defined only for weighted graphs and calculated as the sum of the weights of the neighboring nodes [27], as indicated in Eq. 3.5, where the ω_{ij} is the weight of the connection between the nodes i and j.

$$S_i = \sum_j \omega_{ij} \tag{3.5}$$

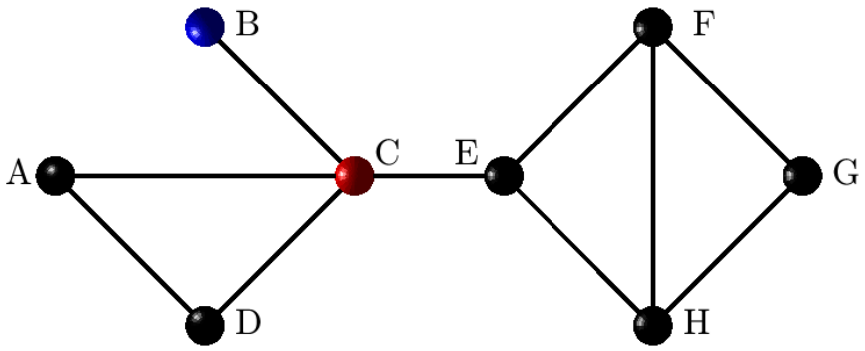

Figure 3.1: Degree of a binary undirected graph. The node C is a node with high degree, $D_C = 1$, and the node B is a node with low degree, $D_B = 1$. Average degree of this graph is 2.5 .

For directed weighted graph the *in-strength*, *out-strength* and strength are calculated similar to the in-degree, out-degree and degree of a directed binary graph. By averaging each of these measures over the whole network, the *average strength*, *average in-strength* and *average out-strength* measures are calculated.

Path length

In a connected graph, i.e. a graph in which every node has at least one neighboring node, there is a link between every pair of nodes via finite number of edges. The length of a link is defined as the number of edges in the pathway between each pair of nodes in the case of binary graphs. However, if the graph is weighted, the length of the link is calculated as the sum of the edges length. Since an edge with higher weight is a stronger connection, its length is considered to be shorter. Therefore, the length of an edge is considered to be inversely proportional to its weight [10].

The link between each pair of nodes which has the lowest length is the shortest pathway between them (Fig. 3.2) and its length is the *distance* — the shortest path length — between those two nodes which is calculated as shown in the Eq. 3.6 for the binary graphs and Eq. 3.7 for the weighted graphs where $k, l \in g(i \longleftrightarrow j)$ indicates the nodes k and l belonging to the shortest pathway between nodes i

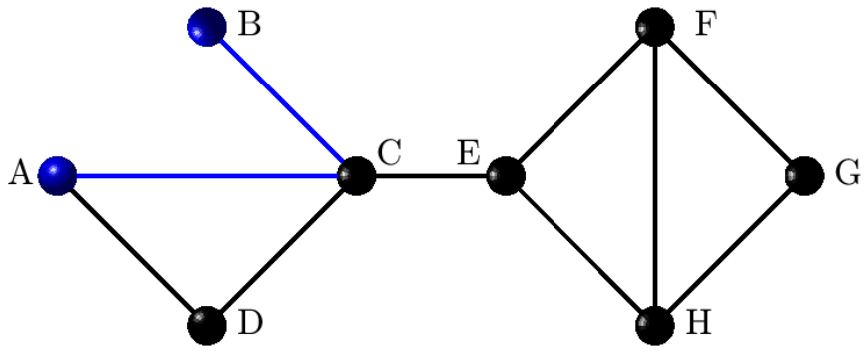

Figure 3.2: The shortest pathway between the nodes A and B. The distance between these two nodes is 2. The radius and diameter, i.e. minimum and maximum eccentricity, of the graph are 2 and 4, respectively.

and j. Note that if there is no possible pathways between two pair of nodes, the distance d_{ij} is considered to be infinite.

$$d_{ij} = \sum_{k,l \in g(i \longleftrightarrow j)} a_{kl} \tag{3.6}$$

$$d_{ij}^{\omega} = \sum_{k,l \in g(i \longleftrightarrow j)} \frac{1}{\omega_{kl}} \tag{3.7}$$

In order to find the shortest pathway different algorithms, for example *Dijkstra's algorithm* for weighted graphs and *breadth-first search* for binary graphs, can be used [28].

The *path length* is the average distance of all nodes from a single node, Eq. 3.8. *In-path length* and *out-path length* are other two nodal measures in directed graphs. The average distances of the source or the destination nodes to or from a single node are defined as in-path length and out-path length, respectively.

$$L_i = \sum_j \frac{d_{ij}}{N-1} \tag{3.8}$$

Characteristic path length (Eq. 3.9), *characteristic in-path length* and *characteristic out-path length* are three global measures which are calculated by averaging the path length, in-path length and out-path length over the whole network.

$$L = \frac{1}{N} \sum_i L_i \tag{3.9}$$

Eccentricity

The *eccentricity* is the maximum distance between a desired node to any other nodes [29], Eq. 3.10. For directed graphs, the maximum incoming and outgoing distances to and from a node are interpreted as *in-eccentricity* and *out-eccentricity*, respectively. Average value of each of these measures gives three global measures, *average eccentricity*, *average in-eccentricity* and *average out-eccentricity*. *Diameter* and *radius* are two other global measures which are the maximum and minimum eccentricity of all nodes, respectively (Fig. 3.2). Note that for disconnected nodes, the eccentricity is set to NaN (Not a Number).

$$E_i = max\{d_{ij}\} \tag{3.10}$$

Triangles

As shown in the figure 3.3, if two neighbors of a single node are also neighbors, these three nodes form a *triangle* [30]. For a binary undirected graph, the number of triangles around a node is calculated by

$$t_i = \frac{1}{2}\sum_{j,k} a_{ij}a_{jk}a_{ki} \tag{3.11}$$

or equivalently

$$t_i = \frac{1}{2}(A^3)_{ii} \tag{3.12}$$

where A is the adjacency matrix. For weighted graphs, however, the calculation of number of triangles is a little different. As shown in 3.13, a geometric mean of the weights contributing to the triangle has to be calculated.

$$t_i = \frac{1}{2}\sum_{j,k}(\omega_{ij}\omega_{jk}\omega_{ki})^{1/3} \tag{3.13}$$

This can be equally calculated by using the reduced weighted matrix

$$\varpi_{ij} = \omega_{ij}^{1/3} \tag{3.14}$$

then

$$t_i = \frac{1}{2}(\varpi^3)_{ii} \tag{3.15}$$

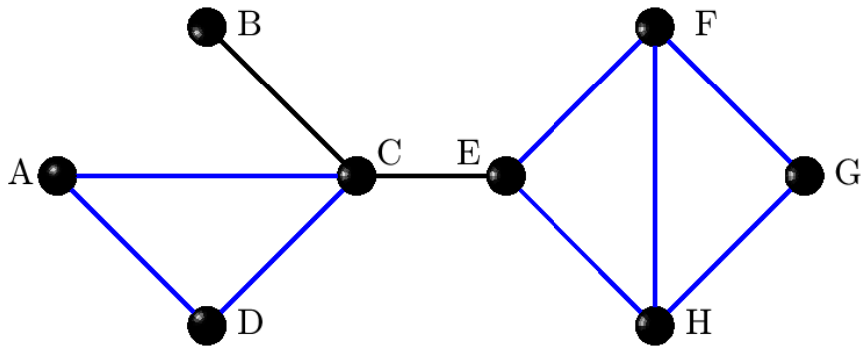

Figure 3.3: Triangles of a binary undirected graph. Since all the neighbors of the node A are also neighbors of each other, its clustering coefficients is 1. However, neighbors of the node H have form only 2 triangles out of the all possible 3. Therefore, its clustering coefficient is $\frac{2}{3}$.

For directed graphs, we only consider a cycle as a triangle and any other kinds of connections forming a triangle are neglected . A cycle is a form of connection in which if $i \to j$ and $j \to k$ then $k \to i$.

Clustering coefficient

Clustering coefficient of a node is equal to the fraction of the triangles around the desired node (Fig. 3.3) [6]. Since the total number of possible triangles around a node of the degree D_i is given by $\binom{D_i}{2}$, clustering coefficient of the node is given by

$$C_i = \frac{2t_i}{D_i(D_i - 1)} \tag{3.16}$$

For directed graphs, the total number of possible triangles around a node is given by

$$D_i^{in} D_i^{out} - D_i^{\leftrightarrow} \tag{3.17}$$

where $D_i^{\leftrightarrow}$ is the false pairs, i.e. pairs that cannot make a triangle such as $i \to j \to i$, which is [31]

$$D_i^{\leftrightarrow} = \sum_{j \neq i} a_{ij} a_{ji} = A_{ii}^2 \tag{3.18}$$

By averaging the clustering coefficient over the whole network the *clustering*

coefficient of the network is found.

Transitivity

Transitivity is a global measure which is calculated as

$$T = \frac{3N_{triangles}}{N_{triples}} \tag{3.19}$$

where $N_{triangles}$ and $N_{triples}$ are the total number of triangles and unordered triples in the graph. $N_{triples}$ is given by [32]

$$N_{triples} = \sum_i D_i(D_i - 1) - D_i^{\leftrightarrow} \tag{3.20}$$

Closeness and betweenness centrality

The *closeness centrality* is calculated as the inverse of the path length — average distance of a node from other nodes — of the desired node. *In-closeness centrality* and *out-closeness centrality* measures are similarly calculated for directed graphs.

Another measure of centrality is the *betweenness centrality* which is a nodal measure calculated as the fraction of the shortest pathways passing through the desired node and is one of the indicators of the **hub** nodes, since these nodes usually have high value of betweenness centrality (Fig. 3.4). In order to calculate this measure, we have used the algorithm proposed by Kintali [33].

Global and local efficiency

Since the efficiency of the information flow is inversely proportional to the distance between two nodes, the *global efficiency* of each node — or simply efficiency — is defined as

$$E_i = \frac{1}{N-1} \sum_j \frac{1}{d_{ij}} \tag{3.21}$$

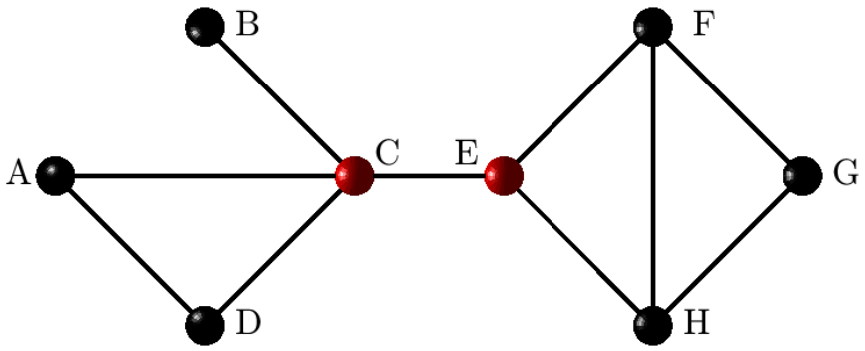

Figure 3.4: Closeness and betweenness centrality of the nodes. Nodes C and E have high closeness and betweenness centrality. These two nodes are the **hubs** of the graph.

for a graph of size N [34]. For a directed graph *in-global efficiency* and *out-global efficiency* are computed in the same manner and the global efficiency is determined as the average of in-global and out-global efficiency. Average values of the above-mentioned measures over the whole graph are considered as another three global measures, also called as global, in-global and out-global efficiency.

The global efficiency of a subgraph consist of every neighbor of a desired node is called *local efficiency*. For weighted graphs, the subgraph is defined as follows

$$\omega'_{j,k} = \sqrt{\sum_{l} \omega_{il}\omega_{li}} \ .\omega_{j,k} \tag{3.22}$$

where j, k and l are neighbors of the node i. Average local efficiency of all nodes gives the local efficiency of the network.

Modularity

A group of nodes that are densely connected with each other but their connections with other nodes are weak, form a **module** (Fig. 3.5). *Modularity* is a measure of how well these modules are segregated relative to a random network [35]. The higher modularity corresponds to stronger connections between nodes of a module and is a sign of better segmentation of the graph into smaller subgraphs. This

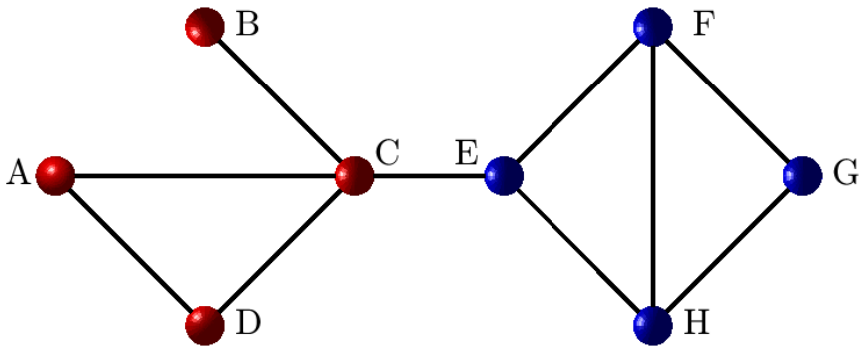

Figure 3.5: Modules of the graph are displayed.

measure is calculated by

$$M = \frac{1}{l}\sum_{i,j}[a_{ij} - \frac{D_i D_j}{l}]s_{ij} \tag{3.23}$$

where s_{ij} is 1 if i and j are in the same module and 0 otherwise and l is the total number of edges in the graph.

Within-module z-score and participation coefficient

In order to quantify how well a node is connected to other nodes of the same module the *within-module z-score* measure is introduced. This measure is calculated as

$$Z_i = \frac{\widetilde{D_i} - \overline{D_{S_i}}}{\sigma_{D_{S_i}}} \tag{3.24}$$

where the $\widetilde{D_i}$ is the degree of the node i inside the module, i.e. number of neighbors the desired node has inside the module, and the $\overline{D_{S_i}}$ and $\sigma_{D_{S_i}}$ are the average degree of the nodes and the standard deviation of the degree within the module S_i, respectively. For the directed graphs the *within-module in-z-score* and *within-module out-z-score* measures are calculated in the same manner.

Another nodal measure similar to within-module z-score is the *participation coefficient* which quantifies how the edges of a node are distributed between

different modules. This measure is represented by

$$P_i = 1 - \sum_{j}^{N_S} (\frac{D_{i,S_j}}{D_i})^2 \tag{3.25}$$

In this equation N_S is the number of modules in the graph and D_{i,S_j} is the number of edges between the node i and the nodes in the module S_j [36]. For instance, the only nodes that have non-zero participation coefficient in the figure 3.5 are the nodes C and E.

Assortativity coefficient

Assortativity coefficient is the measure which quantifies the likelihood of the connection between two nodes of the same degree, e.g. connection between two nodes of the high degree. It is calculated as [37]

$$r = \frac{l^{-1} \sum_{ij} d_i d_j - [l^{-1} \sum_{ij} \frac{1}{2}(d_i + d_j)]^2}{l^{-1} \sum_{ij} \frac{1}{2}(d_i^2 + d_j^2) - [l^{-1} \sum_{ij} \frac{1}{2}(d_i + d_j)]^2} \tag{3.26}$$

which is the correlation between degrees of two nodes at two ends of a vertex.

Small-worldness

In order to functionally specialize different modules, a well-segregated network is required. On the other hand, if functional integration is desired the present of inter-modular connections are inevitable. A network that holds both of these characteristics, i.e. functional segregation and integration, is known as a **small-world** network [10]. In order to a have a small-world network, the network should have a high clustering coefficient but have the same characteristic path length as a random network [6]. Therefore, the *small-worldness* measure is defined by [38]

$$S = \frac{C/C_{rand}}{L/L_{rand}} \tag{3.27}$$

If $S \gg 1$ then the network is considered as a small-world network.

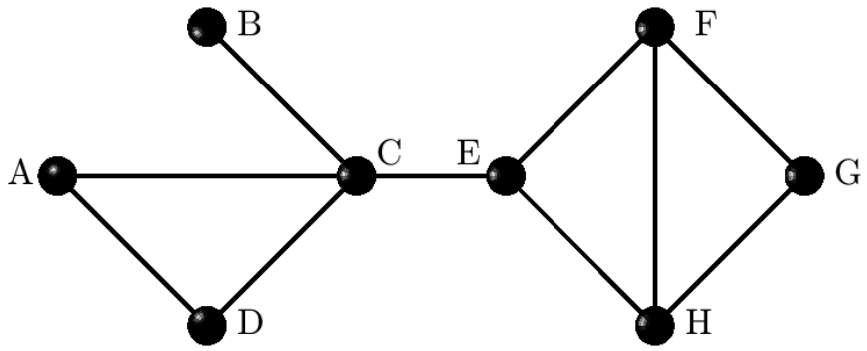

Figure 3.6: A simple binary undirected graph. The nodal measures are calculated and indicated in the table 3.1.

Measure	Node							
	A	B	**C**	D	**E**	F	G	H
Degree	2	1	**4**	2	**3**	3	2	3
Path length	2.29	2.43	**1.57**	2.29	**1.57**	2	2.71	2
Eccentricity	4	4	**3**	4	**2**	3	4	3
Triangle	1	0	**1**	1	**1**	2	1	2
Clustering coefficient	1	0	**0.17**	1	**0.33**	0.67	1	0.67
Closeness	0.44	0.41	**0.64**	0.44	**0.64**	0.50	0.37	0.50
Betweenness	0	0	**28**	0	**24**	5	0	5
Global efficiency	0.56	0.49	**0.76**	0.56	**0.71**	0.64	0.51	0.64
Local efficiency	1	0	**0.17**	1	**0.33**	0.83	1	0.83
Z-score	0	-1.22	**1.22**	0	**-0.87**	0.87	-0.87	0.87
Participation	0	0	**0.38**	0	**0.44**	0	0	0

Table 3.1: Nodal measures calculated for the graph shown in the figure 3.6. Values of the measures for the hub nodes are in bold.

3.2 Statistical analysis

Statistical analysis of the different measurements and comparisons provides information on how significant the results of the analysis are. In this section, some of the statistical tools used in BRAPH are introduced.

P-value

One of the methods used for testing the significance of a measurement is the *hypothesis testing*. In this method, first, a statement is held to be true (*null hypothesis*) [22]. Then a test statistic T_{obs} is calculated for the sample data. Afterwards, the probability of observing values as big or larger than T_{obs} is computed $p = P(T(x) > T_{obs})$. Based on the calculated probability, the null hypothesis can get "rejected" or "accepted". The probability p is called the *p-value* [39].

In BRAPH, to determine whether the between-group comparison and comparison with random graphs are significant or not, the p-value is calculated via a non-parametric permutation test. In the case of between-group comparison, the difference in a graph measure between two groups is calculated. Then, after each permutation the same comparison is made and the p-value is defined as the portion of the histogram with values higher than the value of the initial comparison (Fig. 3.7).

When comparing a graph with random graphs, the p-value is calculated by following the same procedure, except that the value – not the difference – of the measure are compared in the histogram.

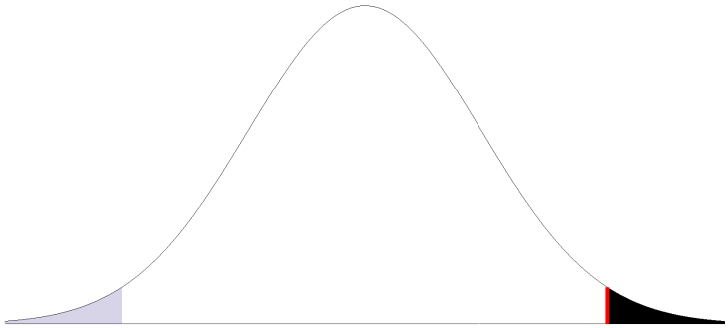

Figure 3.7: The histogram of the values of the comparisons after permutation is illustrated. The red line is the value of the parameter calculated in the initial comparison. The black shaded area shows the extreme values. In the case of one-tailed p-values only this area is important, but for two-tailed p-value, grey shaded area should also be included.

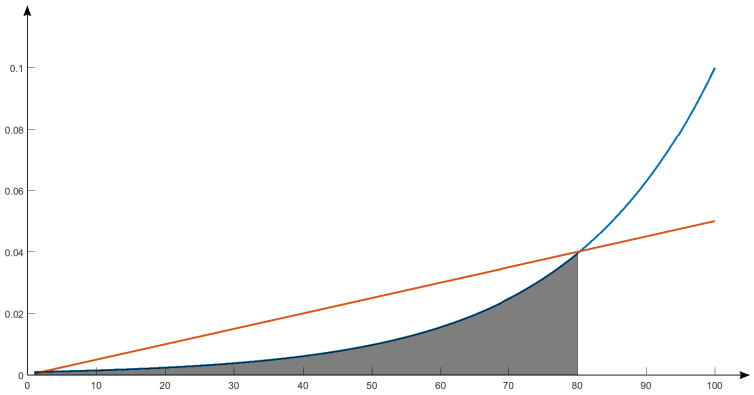

Figure 3.8: The process of the p-value correction due to FDR. Red line shows the $\frac{i}{m}q$. Here the value of the q constant is set to 0.05. The null hypothesis corresponding to the shaded area is rejected, since $p_i \leq \frac{i}{m}q$.

False discovery rate

When a permutation test is done on the nodal measures, the possibility of rejecting the null hypothesis by mistake increases, since multiple permutation tests are done simultaneously on each node. This issue is called *multiple testing problem*. One of the methods of dealing with this error is by correcting the *false discovery*

rate (FDR), which is defined as:

$$FDR = E\left(\frac{V}{R}\right)$$

where the $E\left(\frac{V}{R}\right)$ is the expectation of the ratio of the falsely rejected null hypothesis V to all the rejected null hypothesis R.

To correct p-values according to FDR, first all the calculated p-values should be sorted $p_1 \leq p_2 \leq ... \leq p_m$ where p_i is the p-value corresponding to the null hypothesis H_i. Then, all the null hypothesis whose p-value is less or equal to p_i will be rejected if:

$$p_i \leq \frac{i}{m}q$$

where q is a user-specified constant (Fig. 3.8) [40].

Chapter 4

BRAPH

In this chapter we are going to introduce the different graphical user interfaces (GUIs) in BRAPH and the steps that should be taken to analyze the brain graphs constructed out of the data extracted from various imaging modalities. For more detailed instructions please visit the website www.braph.org [41] .

In general the work-flow (Fig. 4.1) of BRAPH starts from defining the brain regions in the *Brain Atlas* GUI and continues with the *Cohort* GUI to build the cohort by dividing the subjects in different groups. Then the pre-analysis is included to fix the parameters required for the graph analysis, and finally the graph analysis is done based on the type of the graph.

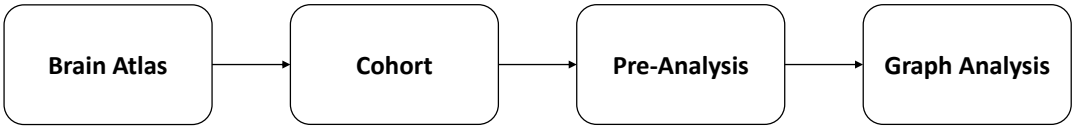

Figure 4.1: The work-flow of BRAPH. First a brain atlas should be defined (**.atlas*), then the cohort of subjects can be built (**.mc* for MRI, **.fc* for fMRI, **.ec* for EEG and **.pc* for PET). Afterwards the pre-analysis should be done to fix the parameters for the graph analysis and finally run the graph analysis(**.mga* for MRI, **.fga* for fMRI, **.ega* for EEG and **.pga* for PET).

4.1 Brain atlas

The *GUIBrainAtlas* (Fig. 4.2) is an interface in which the brain regions are defined based on the parcellation method used in pre-processing the imaging data. This interface provides the ability of creating, editing and loading the brain atlas for users.

To add a brain atlas, the atlas can be imported in txt, xml or xls formats. Before importing a file, it should be prepared in a proper form. The xls files, for example, should be prepared as shown in the figure 4.3. The first row contains the information of the atlas where in the first box the name of the atlas should be indicated and in the second box the brain surface used for visualization of the brain (the brain surface used in BRAPH is based on the ICBM152 template [42]). Starting from the second row, each column corresponds to the label, name, x/y/z-coordinate, hemisphere and note of each brain region, respectively.

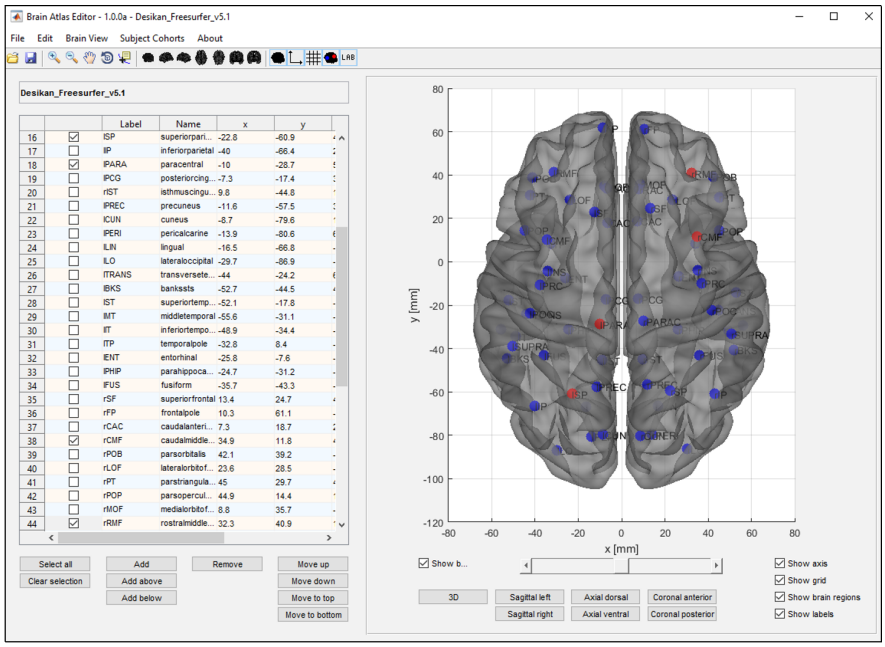

Figure 4.2: Brain atlas graphical user interface.

	A	B	C	D	E	F	
1	Desikan_Freesurfer_v5.1	BrainMesh_ICBM152.nv					
2	lSF	superiorfrontal	-12.6	22.9	42.4	left	.
3	lFP	frontalpole	-8.6	61.7	-8.7	left	.
4	lRMF	rostralmiddlefrontal	-31.3	41.2	16.5	left	.
5	lCMF	caudalmiddlefrontal	-34.6	10.2	42.8	left	.
6	lPOB	parsorbitalis	-41	38.8	-11.1	left	.

Figure 4.3: Proper form of a Brain Atlas in xls format.

In order to customize an atlas, users can add or remove multiple brain regions, change their coordinates and rearrange the list of the regions according to the structure of the data extracted from imaging method in use.

In addition to the tools provided for customizing the brain atlas, some powerful graphical tools are also included to give the user the ability of visualizing the brain in different views (saggital left/right, axial dorsal/ventral, coronal anterior/posterior and 3D).

When the modification of the brain atlas is finalized, the atlas should be saved (in *.atlas format) to allow the user to proceed to the next step.

4.2 Cohort

The cohort GUIs provide the tools required for creating and modifying the groups of subjects and comparing them (only for MRI and PET). This GUIs are slightly different for different imaging techniques. In this section we introduce the GUIs corresponding to MRI and fMRI separately. Please note that the cohort GUIs for EEG and PET are similar to the GUIs for fMRI and MRI, respectively.

MRI

GUIMRICohort (Fig. 4.4) is an interface which provides the required tools for modifying the data and anagraphics of subjects, and grouping the subjects by either adding individual subjects or groups of subjects. In addition between-group comparison is another tool included in this interface which gives the user

the ability to compare the value (e.g. cortical thickness, subcortical volume) assigned to each region between different groups.

Group of subjects can be imported as a single xml, xls or txt file. This file should be prepared in a proper form, as shown in the figure 4.5. The first row (except for the first box, which is the label) contains the names of the brain regions, in the same order as the atlas in use. Starting from the second row, each row contains the data of a single subject with the values assigned to each region written under that region. The first column shows the name (or code) assigned to each subject.

Users can visualize the values assigned to brain regions for different subjects, the average and standard deviation of these values in a specific group and the difference between groups based on the sphere, symbol or label size and color in addition to the sphere transparency. All of these actions are available under the **brain view** menu.

When the cohort is finalized, it should be saved (in *.mc format) to allow the user to start the graph analysis part.

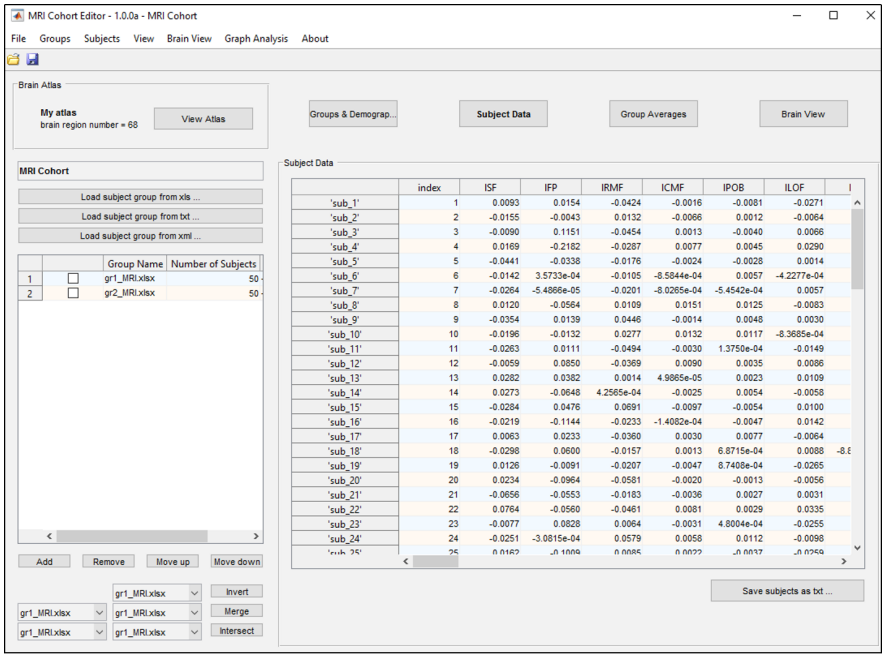

Figure 4.4: MRI Cohort graphical user interface.

	A	B	C	D
1	label	'lh_superiorfrontal_thickness'	'lh_frontalpole_thickness'	'lh_rostralmiddlefrontal_thickness'
2	'sub_1'	9.25E-03	1.54E-02	-4.24E-02
3	'sub_2'	-1.55E-02	-4.32E-03	1.32E-02
4	'sub_3'	-8.98E-03	1.15E-01	-4.54E-02
5	'sub_4'	1.69E-02	-2.18E-01	-2.87E-02
6	'sub_5'	-4.41E-02	-3.38E-02	-1.76E-02

Figure 4.5: Proper form of a group of subjects in xls format for MRI cohort.

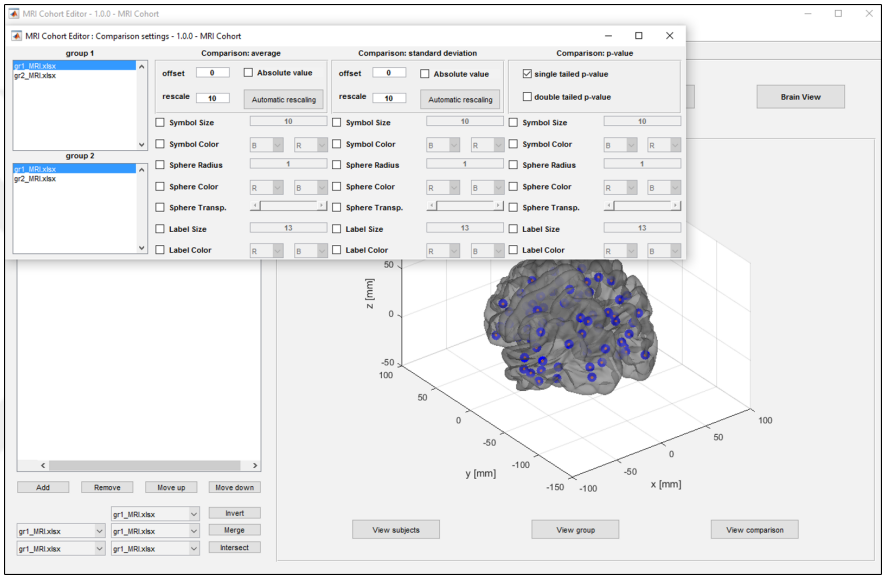

Figure 4.6: Brain view menu for visualization of the data and between-group comparison.

fMRI

GUIfMRICohort (Fig. 4.7) is an interface which also provides the tools for grouping the subjects and modifying the data and anagraphics. However, unlike GUIMRICohort, between-group comparison is not available since the functional data (e.g. absolute value of the BOLD signal) solely does not provide a valid measure for comparison. The subjects can be grouped by either adding individuals to different groups separately or by importing the whole group at once. In order to add a group of subjects, the data files corresponding to subjects of the same group should be included in the same folder (notice that, unlike MRI cohort which has only one data file for each group, fMRI cohort has a folder of data files belonging to each subject for each group).

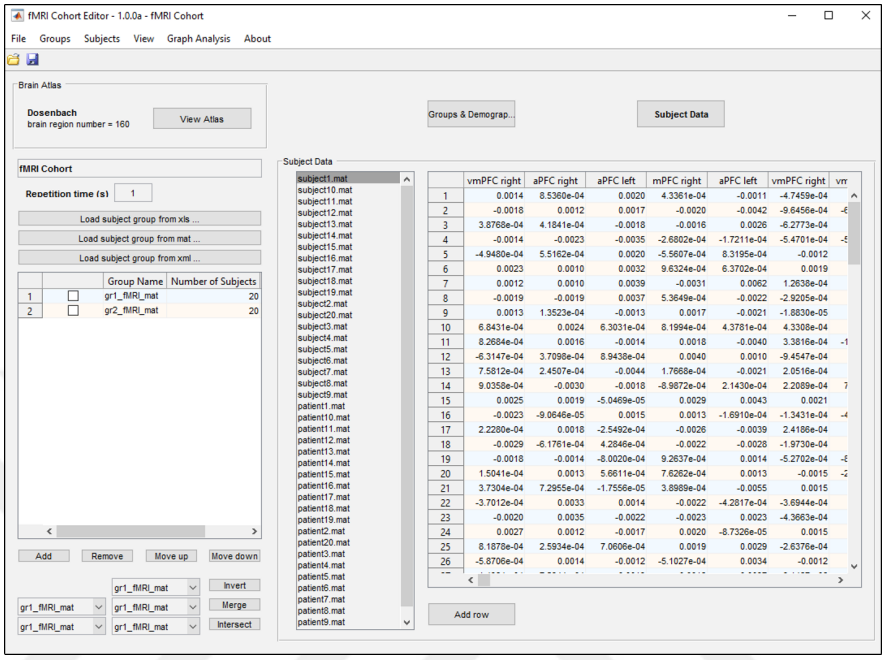

Figure 4.7: fMRI Cohort graphical user interface.

	A	B	C	D	E	F	G
1	0.005617	-0.15421	0.009336	0.012984	0.019246	-0.01743	0.008497
2	0.007112	-0.07111	0.006233	0.017079	0.015981	0.069602	0.011897
3	0.012978	0.073937	0.004542	0.007385	0.026708	0.024005	0.003886
4	0.005961	0.019278	-0.00777	0.009296	-0.02078	0.038691	0.01011
5	0.028241	-0.17635	0.019793	0.018976	-0.01843	-0.00456	0.010796

Figure 4.8: Proper form of a data file of a subject in xls format for fMRI cohort.

The data files for each subject should be in one of the xls, mat or xml formats and they should be prepared in a proper form. As shown in the figure 4.8, each column represents the time series of a single region. The order of regions should be the same as the atlas in use.

When the cohort is finalized, it should be saved (in *.fc format) to allow the user to start the graph analysis part.

4.3 Graph analysis

Graph analysis GUIs of BRAPH provide the tools for constructing the connectivity matrices, calculating the graph measures, comparing the difference between the calculated measures for different groups and the comparison with random networks. These GUIs are built with the consideration of the difference between data types for different imaging modalities. Therefore, each imaging technique has a set of GUIs of its own.

In this section, first the pre-analysis GUIs for MRI and fMRI are introduced. Afterwards, the graph analysis tools for different types of graphs are brought. Please note that the graph analysis GUIs for EEG and PET are similar to the GUIs for fMRI and MRI, respectively.

4.3.1 Pre-analysis

After building the cohort, the first step for analyzing the data using graph theory is constructing the connectivity matrix. Pre-analysis GUIs, like *GUIMRIGraphAnalysis* and *GUIfMRIGraphAnalysis* for MRI and fMRI, give the user the required tools for this purpose. Additionally, they are equipped with community structure detection (modules) and subgraph analysis tools.

Here we are going to present GUIMRIGraphAnalysis and GUIfMRIGraphAnalysis.

MRI

As mentioned before, GUIMRIGraphAnalysis (Fig. 4.9) is an interface designed to give the user the ability of constructing the connectivity matrices, community structure detection and subgraph analysis. In other words, this GUI gets all the needed parameters for starting the graph analysis and passes them to the graph

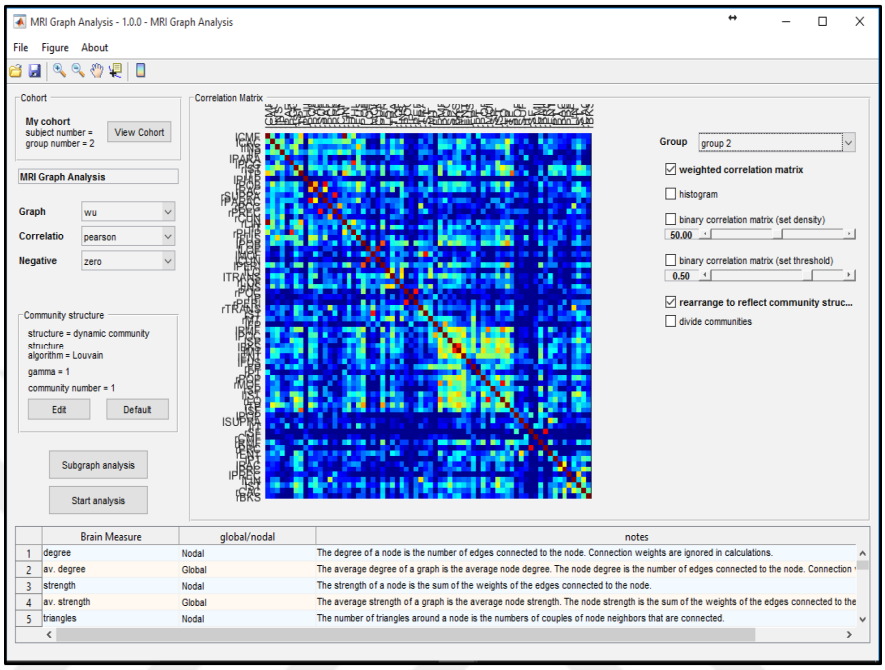

Figure 4.9: MRI pre-analysis graphical user interface.

analysis GUIs.

The main panel of this GUI visually represents the connectivity matrix and the histogram of the weights of the edges. This panel reflects every changes in them caused by the modifications of parameters such as correlation function in use, community structure detection method and threshold and density in the case of binary graphs.

To construct the connectivity matrix for each group, one can select the graph type and different correlation methods – which have been discussed in detail in chapter 2 – included in this GUI. Besides, user can decide how to deal with negative correlation coefficients.

The modules of the graph can be detected and visualized by using a GUI accessible through this interface, which allows the user to choose the community detection algorithm, the resolution parameter, the threshold or density in the case of binary graphs, and fixed or dynamic community structure for graph analysis. When dynamic community structure is chosen the modules are detected for each

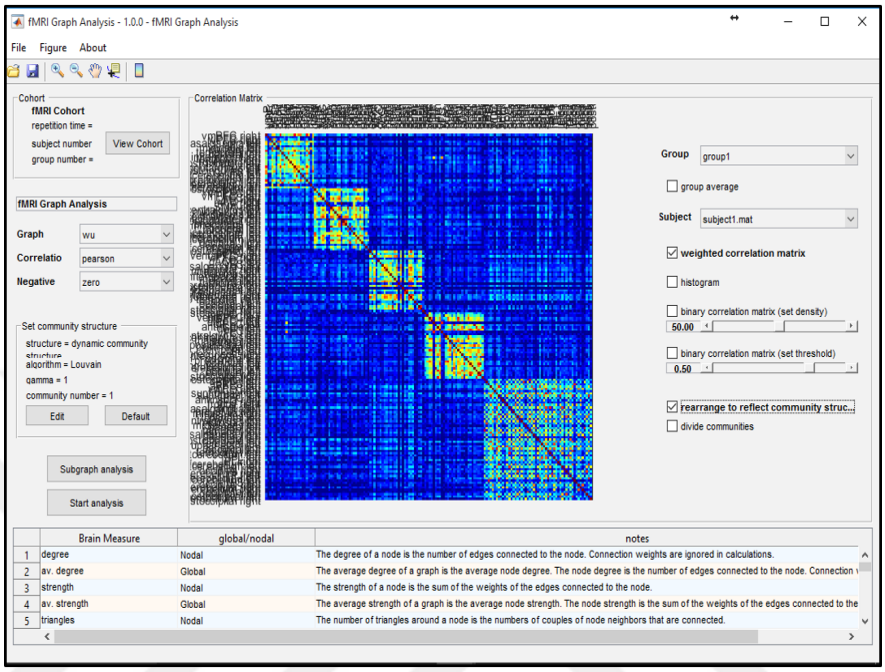

Figure 4.10: fMRI pre-analysis graphical user interface.

connectivity matrix independently. On the other hand, the fixed community structure fixes the modules that have been detected or selected manually and does not change them during the analysis.

In addition to the community detection and connectivity matrix construction, subgraph analysis are also provided which can be achieved by using another GUI accessible through GUIMRIGraphAnalysis. The desired subgraph can be either one of the detected modules or a set of regions selected manually. When the subgraph is selected, it can be analyzed in the same manner of an ordinary graph, by assigning the required parameter via pre-analysis GUI.

fMRI

Just like the pre-analysis GUI for MRI, GUIfMRIGraphAnalysis (Fig. 4.10) has all the required tools for constructing the connectivity matrices, community structure detection and subgraph analysis, and all the procedures for preparing the graphs for analysis are similar. The only difference between these two GUIs is

the fact that every fMRI subject has a single connectivity matrix and the weight of the edges of the connectivity matrix of each group is calculated as the average of the weights of the edges of its subjects.

4.3.2 Analysis

When the pre-analysis of the data are finished, user can advance to the analysis of the graphs. The graph analysis of the data depends on the type of graph (binary or weighted). Therefore, the GUIs for graph analysis of each of these graph types are different. In addition, for binary graphs there are two different GUIs based on the type of thresholding method in use (BUD and BUT).

Here we are going to introduce the user interfaces for graph analysis for weighted and binary graphs. Since the graph analysis GUIs for MRI and fMRI data are just slightly different, we will not discuss them separately.

Analysis of weighted graphs

GUIMRI/fMRI/EEG/PETGraphAnalysisWU (Fig. 4.11) is a user interface that gives the user the power to calculate the graph measures, compare them between different groups and with random networks by permutation test, for weighted graphs. This GUI also provides a very powerful visual representation of the nodal measures.

To calculate each of the graph measures and the comparisons, users have to select the desired measures, then select the type of analysis. By doing so, a specific GUI would appear which allows them to define parameters for analysis. For calculating the measures, after selecting the desired ones, the desired group should be selected. In the case of between-group comparison, the two groups on which the comparison is going to be made, along with the number of permutations should be indicated. If the comparison is longitudinal, the longitudinal checkbox should also be selected.

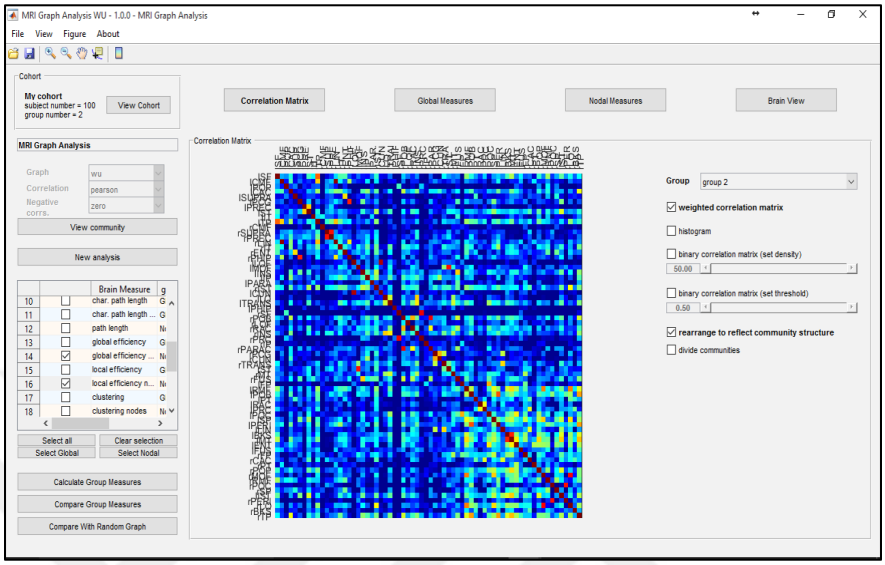

Figure 4.11: Graph analysis graphical user interface for weighted graphs.

If a comparison with random network is desired, the group of subjects, the number of permutations and the number of edges rewiring for randomizing the graph should be indicated.

When the computations are finished, the results are accessible through the tables for global and nodal measures for each group (and for each subject, for fMRI and EEG cases), in which the values of the measures are indicated along with p-value and the upper and lower limits of the confidence interval for random network and between-group comparisons.

In the case of nodal measures, the results can be represented visually by choosing the representation style – the size or color of the symbols, spheres or labels and the transparency of the spheres – as shown in figure 4.12. In the case graph measures, these representations illustrate the value of the measure for each region, while for between-group comparison and random network comparison they show the difference between the values. What's more, the results of the comparisons can be corrected by one-tailed and two-tailed FDR corrections to expose the regions with significantly different value. It is also possible to illustrate both the weighted and binary graphs for each group of subjects.

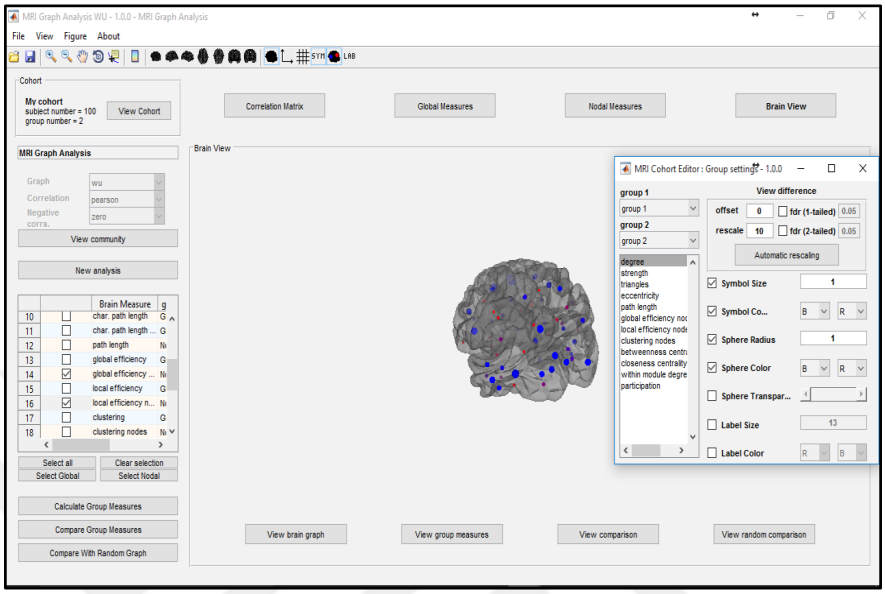

Figure 4.12: Visualization of the analysis results by brain view.

Analysis of binary graphs

GUIMRI/fMRI/EEG/PETGraphAnalysisBUT(BUD) is a user interface that also facilitates the calculation of the graph measures, the comparison between groups and with random networks by permutation test, for binary graphs with fixed threshold (density). The results of the results of the calculations can be visualized for both global and nodal measures, unlike the weighted graphs for which only nodal measures can be visualized.

The process of calculating the measures and comparisons is same as the weighted graphs, except that the threshold (or density) interval and size of the steps should also be indicated. For different thresholds (densities) the values of the calculations are different.

As shown in figure 4.13, BRAPH provides a very useful graphical tool for visualizing the values of the measures and comparisons versus threshold (density) for each group (and for each subject, for fMRI and EEG cases). In addition, confidence interval for comparisons can be also included to give the user an idea of the interval in which the groups show significant difference for different graph

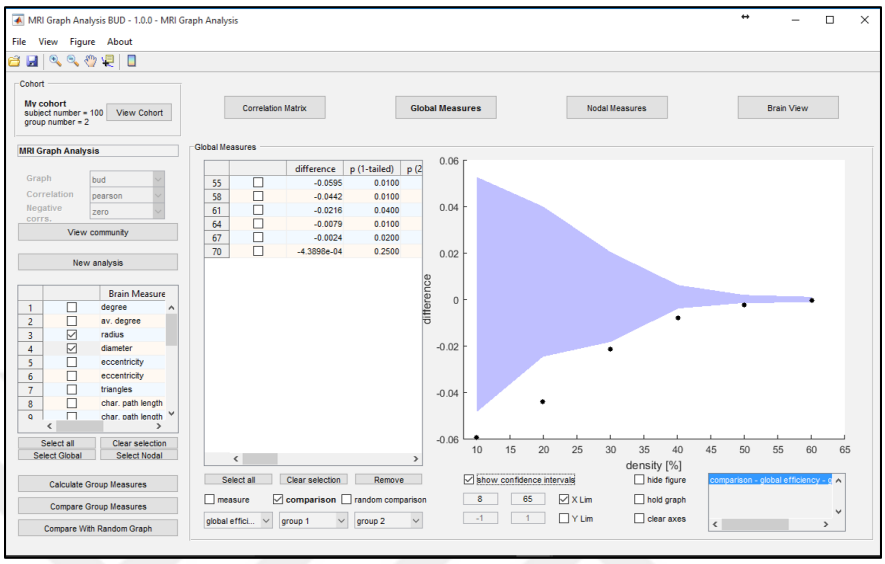

Figure 4.13: Visualization of the analysis results for different densities. The shaded area shows the confidence interval.

measures. The same information is available in the tables for both global and nodal measures.

As discussed for the weighted graphs case, the result of the computations for nodal measures can be visualized in brain view menu by size and color of symbols, spheres and labels and by transparency of the spheres, along with the weighted and binary graphs with different thresholds and densities.

Bibliography

[1] C. G. Gross, *A hole in the head: more tales in the history of neuroscience*. MIT Press Cambridge, MA, 2009.

[2] E. R. Kandel, J. H. Schwartz, T. M. Jessell, S. A. Siegelbaum, and A. J. Hudspeth, *Principles of neural science*, vol. 4. McGraw-hill New York, 2000.

[3] E. Bertin, *A concise introduction to the statistical physics of complex systems*. Springer Science & Business Media, 2011.

[4] T. Nakamura, F. G. Hillary, and B. B. Biswal, "Resting network plasticity following brain injury," *PloS one*, vol. 4, no. 12, p. e8220, 2009.

[5] T. P. Patel, S. C. Ventre, and D. F. Meaney, "Dynamic changes in neural circuit topology following mild mechanical injury in vitro," *Annals of biomedical engineering*, vol. 40, no. 1, pp. 23–36, 2012.

[6] D. J. Watts and S. H. Strogatz, "Collective dynamics of small-worldnetworks," *nature*, vol. 393, no. 6684, pp. 440–442, 1998.

[7] C. J. Stam, "Modern network science of neurological disorders," *Nature Reviews Neuroscience*, vol. 15, no. 10, pp. 683–695, 2014.

[8] J. B. Pereira, M. Mijalkov, E. Kakaei, P. Mecocci, B. Vellas, M. Tsolaki, I. Kłoszewska, H. Soininen, C. Spenger, S. Lovestone, *et al.*, "Disrupted network topology in patients with stable and progressive mild cognitive impairment and alzheimer's disease," *Cerebral Cortex*, p. bhw128, 2016.

[9] J. B. Pereira, D. Aarsland, C. E. Ginestet, A. V. Lebedev, L.-O. Wahlund, A. Simmons, G. Volpe, and E. Westman, "Aberrant cerebral network topology and mild cognitive impairment in early parkinson's disease," *Human brain mapping*, vol. 36, no. 8, pp. 2980–2995, 2015.

[10] M. Rubinov and O. Sporns, "Complex network measures of brain connectivity: uses and interpretations," *Neuroimage*, vol. 52, no. 3, pp. 1059–1069, 2010.

[11] J. Kruschwitz, D. List, L. Waller, M. Rubinov, and H. Walter, "Graphvar: A user-friendly toolbox for comprehensive graph analyses of functional brain connectivity," *Journal of neuroscience methods*, vol. 245, pp. 107–115, 2015.

[12] J. Wang, X. Wang, M. Xia, X. Liao, A. Evans, and Y. He, "Gretna: a graph theoretical network analysis toolbox for imaging connectomics," *Frontiers in human neuroscience*, vol. 9, p. 386, 2015.

[13] M. Xia, J. Wang, and Y. He, "Brainnet viewer: a network visualization tool for human brain connectomics," *PloS one*, vol. 8, no. 7, p. e68910, 2013.

[14] S. Whitfield-Gabrieli and A. Nieto-Castanon, "Conn: a functional connectivity toolbox for correlated and anticorrelated brain networks," *Brain connectivity*, vol. 2, no. 3, pp. 125–141, 2012.

[15] S. H. Hosseini, F. Hoeft, and S. R. Kesler, "Gat: a graph-theoretical analysis toolbox for analyzing between-group differences in large-scale structural and functional brain networks," *PloS one*, vol. 7, no. 7, p. e40709, 2012.

[16] B. He, Y. Dai, L. Astolfi, F. Babiloni, H. Yuan, and L. Yang, "econnectome: A matlab toolbox for mapping and imaging of brain functional connectivity," *Journal of neuroscience methods*, vol. 195, no. 2, pp. 261–269, 2011.

[17] D. B. West *et al.*, *Introduction to graph theory*, vol. 2. Prentice hall Upper Saddle River, 2001.

[18] J. Wang, L. Wang, Y. Zang, H. Yang, H. Tang, Q. Gong, Z. Chen, C. Zhu, and Y. He, "Parcellation-dependent small-world brain functional networks:

a resting-state fmri study," *Human brain mapping*, vol. 30, no. 5, pp. 1511–1523, 2009.

[19] N. Tzourio-Mazoyer, B. Landeau, D. Papathanassiou, F. Crivello, O. Etard, N. Delcroix, B. Mazoyer, and M. Joliot, "Automated anatomical labeling of activations in spm using a macroscopic anatomical parcellation of the mni mri single-subject brain," *Neuroimage*, vol. 15, no. 1, pp. 273–289, 2002.

[20] N. U. Dosenbach, B. Nardos, A. L. Cohen, D. A. Fair, J. D. Power, J. A. Church, S. M. Nelson, G. S. Wig, A. C. Vogel, C. N. Lessov-Schlaggar, *et al.*, "Prediction of individual brain maturity using fmri," *Science*, vol. 329, no. 5997, pp. 1358–1361, 2010.

[21] R. S. Desikan, F. Ségonne, B. Fischl, B. T. Quinn, B. C. Dickerson, D. Blacker, R. L. Buckner, A. M. Dale, R. P. Maguire, B. T. Hyman, *et al.*, "An automated labeling system for subdividing the human cerebral cortex on mri scans into gyral based regions of interest," *Neuroimage*, vol. 31, no. 3, pp. 968–980, 2006.

[22] J. Jobson, *Applied Multivariate Data Analysis: Regression and Experimental Design*. Springer Texts in Statistics, Springer New York, 1999.

[23] R. W. Brown, Y.-C. N. Cheng, E. M. Haacke, M. R. Thompson, and R. Venkatesan, *Magnetic resonance imaging: physical principles and sequence design*. John Wiley & Sons, 2014.

[24] B. Fischl, "Freesurfer," *Neuroimage*, vol. 62, no. 2, pp. 774–781, 2012.

[25] S. A. Huettel, A. W. Song, and G. McCarthy, *Functional magnetic resonance imaging*, vol. 1. Sinauer Associates Sunderland, 2004.

[26] W.-D. Heiss and M. Phelps, *Positron emission tomography of the brain*. Springer Science & Business Media, 2012.

[27] A. Barrat, M. Barthelemy, R. Pastor-Satorras, and A. Vespignani, "The architecture of complex weighted networks," *Proceedings of the National Academy of Sciences of the United States of America*, vol. 101, no. 11, pp. 3747–3752, 2004.

[28] J. Kepner and J. Gilbert, *Graph algorithms in the language of linear algebra*, vol. 22. SIAM, 2011.

[29] J. M. Harris, J. L. Hirst, and M. J. Mossinghoff, *Combinatorics and graph theory*, vol. 2. Springer, 2008.

[30] J.-P. Onnela, J. Saramäki, J. Kertész, and K. Kaski, "Intensity and coherence of motifs in weighted complex networks," *Physical Review E*, vol. 71, no. 6, p. 065103, 2005.

[31] G. Fagiolo, "Clustering in complex directed networks," *Physical Review E*, vol. 76, no. 2, p. 026107, 2007.

[32] M. E. Newman, "Ego-centered networks and the ripple effect," *Social Networks*, vol. 25, no. 1, pp. 83–95, 2003.

[33] S. Kintali, "Betweenness centrality: Algorithms and lower bounds," *arXiv preprint arXiv:0809.1906*, 2008.

[34] V. Latora and M. Marchiori, "Efficient behavior of small-world networks," *Physical review letters*, vol. 87, no. 19, p. 198701, 2001.

[35] M. E. Newman, "Modularity and community structure in networks," *Proceedings of the national academy of sciences*, vol. 103, no. 23, pp. 8577–8582, 2006.

[36] R. Guimera and L. A. N. Amaral, "Cartography of complex networks: modules and universal roles," *Journal of Statistical Mechanics: Theory and Experiment*, vol. 2005, no. 02, p. P02001, 2005.

[37] M. E. Newman, "Assortative mixing in networks," *Physical review letters*, vol. 89, no. 20, p. 208701, 2002.

[38] M. D. Humphries and K. Gurney, "Network small-world-ness: a quantitative method for determining canonical network equivalence," *PloS one*, vol. 3, no. 4, p. e0002051, 2008.

[39] E. D. Kolaczyk, *Statistical analysis of network data : methods and models.* Springer series in statistics, New York ; [London] : Springer, 2009., 2009.

[40] Y. Benjamini and Y. Hochberg, "Controlling the false discovery rate: a practical and powerful approach to multiple testing," *Journal of the royal statistical society. Series B (Methodological)*, pp. 289–300, 1995.

[41] M. Mijalkov, E. Kakaei, J. B. Pereira, E. Westman, and G. Volpe, "Braph: A graph theory software for the analysis of brain connectivity," *bioRxiv*, 2017.

[42] J. C. Mazziotta, A. W. Toga, A. Evans, P. Fox, and J. Lancaster, "A probabilistic atlas of the human brain: Theory and rationale for its development: The international consortium for brain mapping (icbm)," *Neuroimage*, vol. 2, no. 2, pp. 89–101, 1995.